# Structural analysis and sequential resolution for estimation of guaranteed horizons in Partially Observable Petri Nets

Philippe Declerck[1*]

[1*]LARIS, University of Angers, 62 avenue Notre Dame du Lac, Angers, F-49000, France.

Corresponding author(s). E-mail(s): philippe.declerck@univ-angers.fr;

**Abstract**

In Partially Observable Petri Nets, a necessary parameter is the guaranteed horizon, which allows the modelling of the estimation problem with the counter form and can be exploited in estimation for any linear criterion: a problem is the on-line estimation of the guaranteed horizon, which is a maximum sequence length relevant to a sliding horizon or a receding horizon starting from the initial marking. Considering large scale Petri nets, the objective of this paper is to facilitate the resolution by the construction of a triangular form guiding a sequential resolution of the problem based on substructures. This study shows that the classical Dulmage-Mendelsohn decomposition can be applied to a class of Petri nets where the unobservable induced Petri Net is mainly Forward Conflict Free. An extension of this result to any Petri net based on the building of an associated Petri net is made.

**Keywords:** structural analysis, bipartite graph, Petri nets, estimation, sequence, horizon, unobservable transitions

## 1 Introduction

The aim of on-line estimation of optimal current subsequences in Partially Observable Petri Net is to determine firing sequences of unobservable transitions, which are coherent with the observed label sequence produced by the observable transitions and have an optimal value for a criterion, which can present the form of a linear weighting of the transition firing numbers [9] [11]. Various criteria can be treated as the minimum or maximum number of firings in the fault detection presented in [2]. Another criterion is the balance-sheet, that is a global price depending on the costs and gains provided by the tasks [9]. The studies [33] [24] consider the least cost, where each transition has a nonnegative cost in labeled Petri nets. Applications of estimation can be found in fault detection [16] [2], diagnosability [1] [29] [30], estimation for untimed Petri nets [9] and schedulability analysis for P-time Petri nets [4] [10].

In estimation, an interesting objective is that *any possible sequence* can be modelled in the estimation problem on a receding horizon or a sliding horizon. Indeed, as we desire to describe all the sequences and to write a finite set of relations describing the model with the counter form (System (8) in [9]), a horizon which is sufficient large is necessary. Particularly, if the estimation considers an observation relevant to a given finite time, the length of all the possible sequences starting from the initial marking and finishing in this event must also be finite, otherwise, the modelling of the estimation problem is not sufficient to characterize the relevant unobservable sequences [11]. A consequence is that this situation can affect the estimation and the fault detection. This difficulty can arise due to an error modelling, the lack of sensors or inadequate positions of the sensors in the Petri net.

Therefore, the objective is to determine a *majorant* of these horizon lengths relevant to the current observations (in lattice vocabulary, a majorant of a subset is an element not necessarily belonging to the subset, which is greater than any other element of the subset [8]). In addition, a finite majorant brings a useful condition to write a finite set of constraints describing the evolution of the marking and the transition firings [16] [1] [2] [9]. The paper [11] presents a developed motivation of this problem.

However, Petri nets can describe large scale systems as production systems [5] and transportation systems [14], which can limit or even forbid the computation of an estimation approach. Indeed, many estimation approaches consider modest-size systems as they suffer of the state explosion particularly when the estimation tries to determine all the numerical solutions of the state space. Clearly, a computation based on a sequential resolution of smaller subsystems can improve the numerical efficiency of the chosen technique.

In the context of large scale systems, the aim of the paper is the procurement of a partition of the transitions and places in notable sub-structures, which is the support of a sequential estimation. Indeed, the computation (and also the algebraic analysis [11]) in large scale Petri nets can be guided by a structural analysis based on a decomposition of any bipartite graph (and its matrix representation, which is rectangular in general). An interest is the possibility to treat a part of the Petri net even if the consideration of the complete system leads to a state explosion.

The aim is also the establishment of a case study which highlights all the remarkable substructures of the DM decomposition and is usable in a standard paper.

Moreover, an objective is also the improvement of the numerical efficiency of any algorithm applied to the estimation problem in the context of this paper, or potentially outside, in the case of Partially Observable Petri Net defined in this paper. Clearly, the reduction of the size of the subsystems which must be treated directly by an algorithm provides a faster processing and a reduced necessary memory space.

In this paper, we choose the Dulmage-Mendelsohn decomposition (DM decomposition) [17] [18], which has been adapted by different authors for the structural resolution of large scale systems in various fields [26] [28] [12] [7] [6] [27] [11]. The DM decomposition highlights remarkable subsystems as the overdetermined subsystems (roughly speaking,"too many" equations) and the underdetermined subsystems ("too few" equations). Depending of the applications, these subsystems must be desired or avoided. In the field of the simulation of continuous systems, applications are the debugging of software based on modeling languages [6] [27] which focuses on rank deficiencies. [6] works on simple electrical systems while [27] considers different plants as a reduction reactor extracted from a chemical looping process, an iron-based oxygen carrier particle in the presence of methane, and a transient gas pipeline network, which are modeled under a partial differential–algebraic equation system. Performing the Dulmage–Mendelsohn partition on the system of equations resulting from discretizing, this reactor model yields a large square system (1,293 equations $\times$ 1,293 variables), and an over-constrained system (25 equations $\times$ 17 variables) suggesting a difficulty in the modelling of the plant. Another useful field is fault detection in continuous systems, which is based on overdetermined subsystems. The studies [12] [13] are the first papers considering the DM decomposition allowing the computation of a basis of ARRs. Analogous to bond graphs, the study [19] improves this structural approach by taking into account integral and differential causal interpretations for differential constraints. The case study in [19] is an Advanced Water Recovery System which converts waste water to potable water (35 equations $\times$ 33 variables). The research theme treated in [21] is the fault detection and isolation in hybrid systems which are characterized by continuous behaviors that are interspersed with discrete mode changes. Recently, [22] proposes a generalization of the DM decomposition for arbitrary graphs. Considering any triangular form of the unobservable induced subnet of large scale systems, [11] analyzes the RSB property. Contrary to [11], this proposed paper considers not the dual problem but the primal problem and focuses on the applicability of the DM decomposition and the relevant sequential resolution; it highlights a class of unobservable subnets, where the DM decomposition can directly be applied.

Let us complete this short overview by some studies which go beyond automatic control. The paper [35] investigates deadlock control and applies structural analysis techniques, which are based on solving systems of linear algebraic equations. To gain an extra computational speed-up when solving sparse linear systems, a sequential clan-composition process, represented by a weighted graph is examined. The study [31] considers the design of Petri net-based cyber-physical systems as a system containing beverage production and distribution machine. This paper focuses on the splitting of the system into sequential components that can be further implemented as an integrated or distributed system. Employing the p-invariant property, [15] proposes a method for controller synthesis where the original Petri net model is broken down into some smaller models in which the computational cost reduces significantly. The approach is applied to typical production systems and automated guided vehicle systems. In [32], the decomposition into state machine components is made with p-invariant and hypergraph theory, both methods having their advantages and disadvantages.

In this paper, we assume the following assumptions for the different Petri nets under investigation:

- Assumption $\mathcal{AS}-1$ : the incidence matrices and the initial marking (denoted $M^{init}$ below) are known.

- Assumption $\mathcal{AS}-2$ : the Petri net is live.

- Assumption $\mathcal{AS}-3$ : the firing number of some transitions (observable transitions) is known while the current marking of all places is unknown.

- Assumption $\mathcal{AS}-4$ : the firing number of each observable transition is finite.

- Assumption $AS-5$ : the observations are distinguishable, that is, the same label cannot be associated with more than one observable transition ([2] considers the estimation problem and not the structural analysis for the case of indistinguishable events).

- Assumption $AS-6$ . A unique firing of a transition on all transitions occurs at each time.

**Remark.** Assumption $\mathcal{AS}-3$ implies that partially observable Petri nets, where the transitions are partially observable and the places are unobservable, are only considered in the paper. The structural analysis of partially observable places and transitions is a perspective.

**Remark.** Assumption $AS-6$ is a facility to express the sequences under a form without concurrency. A close notion is the single server semantics clearly presented in [24]: if a transition indicates an operation capable of executing by a single server in T-time Petri nets, a transition may only fire once at a time, regardless of its enabling degree. In Assumption $AS-6$ , a transition may only fire once at a time and moreover, the firings of two transitions cannot be simultaneous.

The assumption of boundedness of the marking and the hypothesis of acyclicity are not considered in this article contrary to many papers in this topic: the Petri nets in the examples can present circuits and self-loops. To facilitate the presentation, we consider that a software (Matlab, GNU Octave,...) making a permutation of the rows and columns of the induced unobservable Petri net has built the canonical decomposition given in the different tables. The algorithms of maximum matching as the classical "Hungarian method" (developed by H. Kuhn) and the algorithm of permutation of the rows and columns of a matrix [26] [28] leading to its DM decomposition are out the scope of the paper. As the paper focuses on the sequence length, the state estimation studied in many references is out the scope of this paper [16] [2] [23] [9] [3] [10].

The paper is organized as follows. Section 2 gives the preliminary notations while Section 3 describes the principle of the computation of guaranteed horizons and focuses on receding horizons. This principle is exploited and developed under a structural point of view in Section 4, which considers the determination of the substructures of the unobservable induced Petri Net. Generalizing the applicability of this technique, Section 5 is based on the construction of an associated Petri net close to the initial one, which can be decomposed with the DM decomposition. The on-line sequential resolution based on the substructures is discussed in Section 6. In the context of continuous systems, Appendix 1 in Section 9 illustrates the DM resolution and the relevant resolution with a simple electrical system. The efficiency of the off-line decomposition is discussed in Section 5.4 while Section 7 analyzes the limitations of the approach.

## 2 Preliminary notations

### 2.1 Notations for Petri nets

The entry in the $i-th$ row and $j-th$ column of a matrix $A$ is denoted $A(i,j)$. The notation $A(i,.)$ represents the row $i$ of $A$ while $A(.,j)$ expresses the column $j$. The notation $|Z|$ is the cardinality of set $Z$ and the notation $A^T$corresponds to the transpose of matrix $A$. Symbol $\setminus$ is the set difference, that is, $U \setminus V$ is the set formed by the elements of set $U$ that are not in set $V$. The 1-norm of vector $u$ is equal to the sum of the absolute values of the vector elements and is denoted $\parallel u \parallel_1$ . The notation $\lfloor x \rfloor$ represents the greatest integer less than or equal to $x$. A Place/Transition (P/TR) net is the structure $N = (P, TR, W^+, W^-)$, where $P$ is a set of $|P|$ places and $TR$ is a set of $|TR|$ transitions. The matrices $W^+$ and $W^-$ are respectively the $|P| \times |TR|$ post and pre-incidence matrices over $\mathbb{N}$, where each row $l \in \{1, ..., |P|\}$ specifies the weight of the incoming and outgoing arcs of the place $p_l \in P$. The incidence matrix is $W = W^+ - W^-$. The preset and postset of the node $v \in P \bigcup TR$ are denoted by ${}^\bullet v$ and $v^\bullet$, respectively. A source transition $tr_i \in TR$ satisfies ${}^\bullet tr_i = \emptyset$. The notation $\Omega^*$ represents the set of firing sequences, denoted $\sigma$, consisting of transitions of the set $\Omega \subset TR$. The vector $\overline{\sigma}$ of dimension $|TR|$ expresses the firing vector or count vector of the sequence $\sigma \in TR^*$, where the $i$-th component $\overline{\sigma_i}$ is the firing number of the transition $tr_i \in TR$, which is fired $\overline{\sigma_i}$ times in the sequence $\sigma$. A source transition $tr_i \in TR$ satisfies ${}^\bullet tr_i = \emptyset$ and its firing count can be infinite.

The marking of the set of places $P$ is a vector $M \in \mathbb{N}^{|P|}$ that assigns to each place $p_i \in P$ a non-negative integer number of tokens $M_i$, represented by black dots. The $i$-th component $M_i$ is also written $M(p_i)$. The marking $M$ reached from the initial marking $M^{init}$ (which replaces the usual notation $M_0$) by firing the sequence $\sigma$ can be calculated by the fundamental relation: $M = M^{init} + W.\overline{\sigma}$. The transition $tr$ is enabled at $M$ if $M \geq W^-(., tr)$ and may be fired yielding the marking $M' = M + W(., tr)$. We write $M[\sigma \succ$ to denote that the sequence of transitions $\sigma$ is enabled at $M$, and we write $M[\sigma \succ M'$ to denote that the firing of $\sigma$ yields $M'$. To easily describe the Petri net with incidence matrices, we assume that there is at most a unique arc between a place $p_l$ and each input (resp. output) transition $x_i$ of this place: each weight $(W)^+_{l,i} \neq 0$ ( respectively, $(W)^-_{l,i} \neq 0$) corresponds to a unique arc. Otherwise a simple modification of the Petri net yields the desired form.

### 2.2 Notations for estimation

Remember that only transitions are partially observable: a labeling function $L : TR \rightarrow AL \cup \{\varepsilon\}$ assigns to each transition $tr \in TR$ either a symbol from a given alphabet $AL$ or the empty string $\varepsilon$. In a partially observed Petri net, we assume that the set of transitions $TR$ can be partitioned as $TR = TR_{obs} \bigcup TR_{un}$, where the set $TR_{obs}$ (respectively, $TR_{un}$) is the set of observable transitions associated with a label of $AL$ (the empty string $\varepsilon$). In this paper, we assume that the same label of $AL$ cannot be associated with more than one transition of $TR_{obs}$ (Assumption $AS-5$ ).

The $TR_{un}-$induced subnet of the Petri net $N$ is defined as the new net $N_{un} = (P, TR_{un}, W^+_{un}, W^-_{un})$, where $W^+_{un}$ and $W^-_{un}$ (respectively, $W^+_{obs}$ and $W^-_{obs}$) are the restrictions of $W^+$ and $W^-$ to $P \times TR_{un}$ (respectively, $P \times TR_{obs}$). This unobservable subnet of the Petri net is also named Unobservable Induced Petri Net (UIPN). Therefore, $W_{un} = W^+_{un} - W^-_{un}$ (respectively, $W_{obs} = W^+_{obs} - W^-_{obs}$). A reorganization of the columns with respect to $TR_{un}$ and $TR_{obs}$ yields $W = \begin{pmatrix} W_{un} & W_{obs} \end{pmatrix}$. The following notion of Forward Conflict Free (FCF) is adapted to the UIPN: the UIPN is FCF, i.e., any two distinct unobservable transitions have no common input place (formally, $|(p_l^{\bullet} \cap TR_{un})| \leq 1$ for any place $p_l$).

Notation $x_i$ expresses an unobservable transition, belonging to $TR_{un}$ while an observable transition belonging to $TR_{obs}$ is denoted $y_i$. The notation of the count vectors is taken for $\overline{x}$ of dimension $|TR_{un}|$ and $\overline{y}$ of dimension $|TR_{obs}|$. The reorganization of the components of $\overline{\sigma}$ yields $\overline{\sigma} = \begin{pmatrix} \overline{x}^T & \overline{y}^T \end{pmatrix}^T$.

Starting from the marking $M^{<1>}$, which is the initial marking $M^{init}$ at time zero, the estimation of the current unobservable sequence is based on the treatment of the data produced by the observed transitions successively in an on-line procedure. Notation $\overline{x}^{<k>}$ represents the count vector for the unobservable transitions $TR_{un}$ for step $< k >$ separating two successive observations for $k \geq 2$. From $M^{<k>}$, the transition firings relevant to $\overline{x}^{<k>}$ and $\overline{y}^{<k>}$ allow the establishment of marking $M^{<k+1>}$ : formally, $M^{<k>}[\sigma^{<k>} \succ M^{<k+1>}$ such that $\overline{\sigma}^{<k>} = \begin{pmatrix} (\overline{x}^{<k>})^T & (\overline{y}^{<k>})^T \end{pmatrix}^T$. As $M^{<1>}$ is the initial marking, we assume that $\overline{x}^{<k>} = 0$ and $\overline{y}^{<k>} = 0$ for $k \leq 0$. So, the estimation limited to one step must consider $M^{<1>}[x^{<1>}y^{<1>} \succ M^{<2>}$ for step $< 1 >$, then $M^{<2>}[x^{<2>}y^{<2>} \succ M^{<3>}$ for step $< 2 >$ and so on. The generalization to a horizon composed of several steps is immediate. Note that *these notations are not cumulative* as we can have $\overline{x}^{<3>} = 0$ but $\overline{x}^{<1>} \neq 0$ and $\overline{x}^{<2>} \neq 0$ : the condition $\overline{x}^{<1>} \leq \overline{x}^{<2>} \leq \overline{x}^{<3>}$ does not hold. The notations $\overline{x}^{<0>\to<k>} = \sum_{k'=0,\ldots,k} \overline{x}^{<k'>}$ and $\overline{y}^{<0>\to<k>} = \sum_{k'=0,\ldots,k} \overline{y}^{<k'>}$ allow to write shorter expressions.

# 3 Guaranteed horizons

## 3.1 Guaranteed horizon for a sliding horizon

In this section, the objective is to determine a guaranteed horizon (in other words, a majorant of the sequence lengths) such that any possible sequence $x^{<k>}y^{<k>}$ of the Petri net can be expressed for step $< k >$ when the sequence of the observed firing events of the transitions of $TR_{obs}$ is known. So, the sliding horizon is limited to a unique step in this section. With that aim, we consider the greatest possible length of any unobservable sequence $x^{<k>}$ which is the worst case in terms of number of firings for the unobservable transitions when Assumption $AS-6$ is taken. Consequently, a guaranteed horizon denoted $h_g^{<k>}$ for step $< k >$ and its relevant sequence $x^{<k>}y^{<k>}$, is given by $h_g^{<k>} = \max \parallel \overline{x}^{<k>} \parallel_1 +1$, where 1 corresponds to the unique observation expressed in $y^{<k>}$ (Assumption $AS-6$ ). Consequently, the modelling of the estimation problem on a sliding horizon reduced to $< k >$ can exploit this parameter to characterize all the unobservable sequences and to treat the estimation problem for any criterion [9]. Note that the determination of the guaranteed horizon takes a pessimistic point of view: if Assumption $AS-6$ is removed, concurrency is possible and

**Table 1** Main notations

| Notation | Description |
|---|---|
| $P$ | Set of places $p_i \in P$ |
| $TR$ | Set of transitions $tr_j \in TR$ |
| $TR_{obs}$ | Set of observable transitions $y_i \in TR_{obs}$ |
| $TR_{un}$ | Set of unobservable transitions $x_i \in TR_{un}$ |
| $W$ | Incidence matrix |
| $W^+$ (resp. $W^-$) | Post-incidence matrix (resp. pre-incidence matrix) |
| $W_{un}$ | Incidence matrix of the unobservable induced subnet |
| $W(i,.)$ | Row $i$ of $W$ |
| $W(.,j)$ (resp. $W(.,tr_j)$) | Column $j$ of $W$ (resp. column of transition $tr_j$) |
| $M_i$ | Marking of place $p_i$ with $i \in \{1,\ldots,\lvert P\rvert\}$ ($M_i = M(p_i)$) |
| $M^{init}$ | Initial marking ($M_3^{init}$: initial marking of place $p_3$) |
| $< k >$ | Step k of the estimation |
| $M^{<k>}$ | Marking at step $< k >$ ($M^{<1>}= M^{init}$) |
| $x^{<k>}$ (resp. $y^{<k>}$) | Subsequence relevant to the unobservable transitions at step $< k >$(resp. observable transitions) |
| $\overline{x}^{<k>}$ (resp. $\overline{y}^{<k>}$) | Count vectors of $x^{<k>}$ (resp. $y^{<k>}$) |
| $\overline{x}^{<0>\to<k>}$ (resp. $\overline{y}^{<0>\to<k>}$) | Sum of $\overline{x}^{<k>}$ (resp. $\overline{y}^{<k>}$) on horizon $\{0, 1, \ldots, k\}$ |
| $\lVert \overline{x}^{<k>} \rVert_1$ | Length of sequence $x^{<k>}$ |
| $C$ | Matching in the bipartite graph |
| $S^>, S^=, S^<$ | Canonical subtructures |

sequences having smaller lengths can be obtained. The following relations (1) and (2) are simplified descriptions of the estimation problem as the firing conditions of the unobservable transitions are neglected. The advantage is the fixed dimensions of the matrices, which only depend on the numbers of places and transitions of the Petri net. Relations (1) and (2) are deduced from the firing of an observable transition occurring at the end of step $< 1 >$ and $< k >$ respectively.

For step $< k = 1 >$, the optimization $max(c.\overline{x}^{<1>}) = \max \lVert \overline{x}^{<1>} \rVert_1$ with $c_{1\mathrm{x}|TR_{un}|}$ unitary for the system [9]

$$-W_{un}.\overline{x}^{<1>} \leq b^{<1>} \tag{1}$$

with $\overline{x}^{<1>} \geq 0$ and $b^{<1>} = M^{<1>} - W^-_{obs}.\overline{y}^{<1>}$ gives a majorant relevant to the unobservable transitions, and so a guaranteed horizon $\max \lVert \overline{x}^{<1>} \rVert_1 + 1$ for the sequence $x^{<k>}y^{<k>}$.

For the following steps $k \geq 2$, a possible simplified system [9] is

$$\begin{pmatrix} -W_{un} & 0 \\ -W_{un} & -W_{un} \end{pmatrix} \cdot \begin{pmatrix} \overline{x}^{<0>\to<k-1>} \\ \overline{x}^{<k>} \end{pmatrix} \leq \begin{pmatrix} M^{<1>} + W_{obs} \cdot \overline{y}^{<0>\to<k-1>} \\ b^{<k>} \end{pmatrix} \tag{2}$$

with $\overline{x}^{<0>\to<k>} \geq 0$ and $b^{<k>} = M^{<1>} + W_{obs} \cdot \overline{y}^{<0>\to<k-1>} - W^-_{obs}.\overline{y}^{<k>}$.

**Theorem 1.** *[9] The following optimization*

$$\nabla^{<k>}_{\max} = \max \lVert \overline{x}^{<k>} \rVert_1$$

*for constraints (1) or (2), where $x^{<k>}$ represents the unobservable sequence of the untimed Petri net for step $< k >$, defines a guaranteed time horizon*

$$h_g^{<k>} = \nabla_{\max}^{<k>} + 1 \tag{3}$$

*for any sequence if $\nabla_{\max}^{<k>}$ is finite.*

**Example 1**

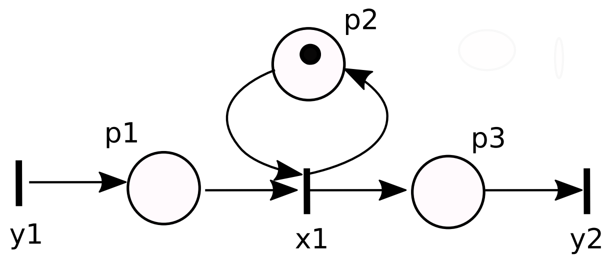


**Fig. 1** Elementary Petri net 1 (example 1)

Let us consider the elementary Petri net 1 of Fig. 1. We have: $P = \{p_1, p_2, p_3\}$; $TR = TR_{obs} \bigcup TR_{un}$ with $TR_{obs} = \{y_1, y_2\}$ and $TR_{un} = \{x_1\}$. So, $W_{obs} = \begin{pmatrix} 1 & 0 \\ 0 & 0 \\ 0 & -1 \end{pmatrix}$ and $W_{un} = \begin{pmatrix} -1 \\ 0 \\ 1 \end{pmatrix}$. For the observation sequence $y_1y_2$, the resolution of (1) directly gives $\overline{x}_1^{<1>} = 0$ for step $< k = 1 >$ (no firing of $x_1$ before observation $y_1$) and $\nabla_{\max}^{<1>} = 0$. The resolution of (2) yields $\overline{x}_1^{<1>} + \overline{x}_1^{<2>} = 1$ for step $< k = 2 >$ (firing of $x_1$ at step $< 1 >$ or $< 2 >$ before observation $y_2$) and $\nabla_{\max}^{<2>} = 1$. As this example is elementary, we can immediately deduce that the system follows the unique sequence $y_1x_1y_2$. These results are obtained despite that the self-loop is not represented in the incidence matrix $W_{un}$ contrary to $W_{un}^+$ and $W_{un}^-$. Now, the consideration of all the relations describing the Petri net for step horizons $\{< 0 >, < 1 >\}$ and $\{< 0 >, < 1 >, < 2 >\}$ (the firing conditions of $x_1$ are also considered) confirms the obtained majorants $\nabla_{\max}^{<1>}$ and $\nabla_{\max}^{<2>}$. ■

## 3.2 Guaranteed horizon for a receding horizon

In this section, we consider the receding horizon going from $< 0 >$ to $< k >$ where the Integer Linear Programming problem (ILP problem) is

$$max(c.\overline{x}^{<0>\to<k>}) \text{ such that} \tag{4}$$

$$-W_{un}.\overline{x}^{<0>\to<k>} \leq b^{<k>} \tag{5}$$

with $\overline{x}^{<0>\to<k>} \geq 0$ over $\mathbb{Z}$ and $b^{<k>} = M^{<1>} + W_{obs} \cdot \overline{y}^{<0>\to<k-1>} - W_{obs}^{-} . \overline{y}^{<k>}$ for the succession of steps going from $< 0 >$ to $< k >$.

Note that (5) corresponds to the second line of (2) and inequality (1) as for $k = 1$, $\overline{x}^{<0>\to<1>} = \overline{x}^{<0>} + \overline{x}^{<1>} = \overline{x}^{<1>}$ and $b^{<1>} = M^{<1>} + W_{obs} \cdot \overline{y}^{<0>\to<0>} - W_{obs}^{-}.\overline{y}^{<1>} = M^{<1>} - W_{obs}^{-}.\overline{y}^{<1>}$ since $\overline{y}^{<0>\to<0>} = \overline{y}^{<0>} = 0$.

Assuming the convergence of the optimization [9], we introduce the following result where the ILP problem (4-5) is relaxed over $\mathbb{R}$. Symbol $h_g^{<0>\to<k>}$ represents a guaranteed receding horizon relevant to the succession of steps going from $< 0 >$ to $< k >$.

**Theorem 2.** *Let us assume that the space defined by (5) over $\mathbb{R}$ is non-empty. For the succession of steps going from $< 0 >$ to $< k >$, a guaranteed horizon is $h_g^{<0>\to<k>} = \lfloor c.\overline{x}_{opt}^{<0>\to<k>} \rfloor + k$, where $\overline{x}_{opt}^{<0>\to<k>}$ is the result of the optimization (4-5) relaxed over $\mathbb{R}$.*

**Proof.**

If $\max_{\mathbb{R}}(c.\overline{x}^{<0>\to<k>})$ in the relaxed problem is finite, the same conclusion holds for the ILP problem, which is more restrictive. Formally, $\max_{\mathbb{N}}(c.\overline{x}^{<0>\to<k>}) \leq \max_{\mathbb{R}}(c.\overline{x}^{<0>\to<k>})$. So, $\lfloor c.\overline{x}_{opt}^{<0>\to<k>} \rfloor$ gives a majorant of $c.\overline{x}^{<0>\to<k>}$ over $\mathbb{N}$ for (5). Variable $k$ in the expressions corresponds to the $k$ observations $y^{<k>}$ for the succession of steps going from $< 0 >$ to $< k >$ under Assumption $AS - 6$ . ■

Considering the computed horizon in a state estimation, we can build a system using the firing conditions of the transitions and the marking equation such as [16] [1] and make an optimization [2] [9]. However, the guaranteed horizon $h_g^{<0>\to<k>}$ increases with $k$, which is a drawback as an excessively large horizon can prevent the computation of a consistent sequence satisfying the firing conditions of the Petri net. But, this numerical limitation is not about $\lfloor c.\overline{x}_{opt}^{<0>\to<k>} \rfloor$, which can always be computed (under a condition presented in [9]). Moreover, this difficulty disappears if the estimation on a receding horizon $\{< 0 >, < 1 >, \ldots, < k >\}$ is replaced by an estimation on a sliding horizon $\{< k - K >, < k - K + 1 >, \ldots, < k >\}$, where $K$ is the step horizon ($K + 1$ is the number of considered steps). In that case, the guaranteed horizon $h_g^{<k>} = max(c.\overline{x}^{<k>}) + 1$ for each step $< k >$ must be computed with Theorem 1.

# 4 DM decomposition for FCF UIPNs

## 4.1 Introduction

In this part, the analysis is based on the synthetic form (5) optimized with (4) presented in Section 3.2. Indeed, it presents the general form $max(\boldsymbol{c}.\boldsymbol{x})$ such that $\boldsymbol{A}.\boldsymbol{x} \leq \boldsymbol{b}$ where each component of the variable $\boldsymbol{x}$ and its relevant column in $\boldsymbol{A}$ corresponds to an unobservable transition: this correspondence will facilitate the analysis. To alleviate the notations, we replace $\overline{x}^{<0>\to<k>}$ by $\overline{x}$ in the sequel. As the resolution considers the unknown variables, we separate the transitions of $TR$ in two sets:

- The set of observable transitions $TR_{obs}$, which correspond to the known variables $\overline{y}$.

- The set of unobservable transitions $TR_{un}$, which are relevant to unknown variables $\overline{x}$.

Let us present the objective of this part by introducing the following result and Example 2.

**Theorem 3.** *The problem (4-5) is upper-bounded, if and only if, all the components $\overline{x}_i$ are upper-bounded.*

**Proof.** 1) If $max(c.\overline{x})$ with $c$ unitary in the problem (4-5) is upper-bounded, necessary each component $\overline{x}_i$ must also be upper-bounded. Indeed, we can consider the converse of this original assertion. If a variable $\overline{x}_i$ is not upper-bounded, that is, $max(c_i.\overline{x}_i) = +\infty$ with $c_i = 1 > 0$, then $max(c.\overline{x})$ is also not upper-bounded: the guaranteed horizon cannot be defined on the complete system for any criterion. 2) Conversely, if all the components $\overline{x}_i$ are upper-bounded, then $max(c.\overline{x})$ with $c$ unitary is clearly upper-bounded. ■

However, the analysis of some examples as Example 2 below shows that this optimization can still be made on subsystems even if it is impossible for the complete system. Therefore, the objective is to determine the subsystems of the large scale system and to make a sequential resolution following these blocks.

**Example 2.**

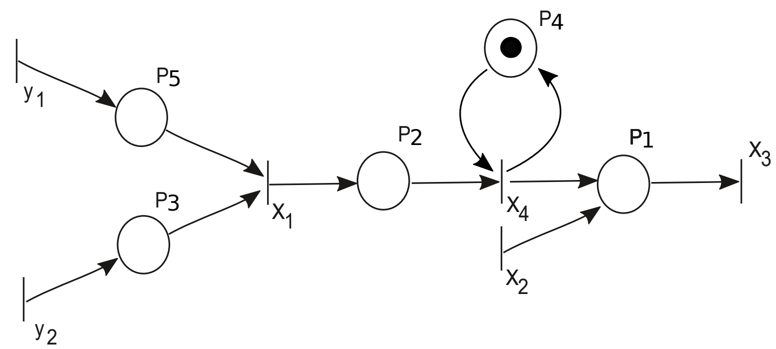


**Fig. 2** Elementary Petri net 2 (example 2)

Let us consider the elementary Petri net 2 of Fig. 2. We have: $P = \{p_1, p_2, \ldots, p_5\}$; $TR = TR_{obs} \bigcup TR_{un}$ with $TR_{obs} = \{y_1, y_2\}$ and $TR_{un} = \{x_1, x_2, x_3, x_4\}$. The source transitions $y_1$ and $y_2$ are observable while the source transition $x_2$ is unobservable. The incidence matrix at the top of Table 2 does not suggest a clear resolution despite that the Petri net is simple. However, a reorganization of the places and transitions leads to the second matrix at the bottom of Table 2, where a resolution can easily be established by following the new order of the transitions and places from the left upper part to the right lower part. Indeed, the firing number $\overline{x}_1$ can be upper-bounded by two ways: $y_1$ through $p_5$ and $y_2$ through $p_3$ ( $\overline{x}_1 \leq M_5 + \overline{y}_1$ and $\overline{x}_1 \leq M_3 + \overline{y}_2$). The firing number $\overline{x}_4$ can be upper-bounded with only one way: $x_1$ through $p_2$ ($\overline{x}_4 \leq M_2 + \overline{x}_1$); the self-loop with $p_4$ cannot be exploited as the relevant row is null. The firing number $\overline{x}_3$ cannot be upper-bounded through $p_1$ as $x_2$ is unobservable ($\overline{x}_3 \leq M_1 + \overline{x}_4 + \overline{x}_2$). These three cases of resolution lead to a partition of the unobservable transitions and define three cases of substructures highlighted in grey. Finally, an upper bound can be provided for $\overline{x}_1$ and $\overline{x}_4$ but not for $\overline{x}_3$ and $\overline{x}_2$. ■

**Table 2** Two incidence matrices of the same Petri net 2

| | $y_1$ | $y_2$ | $x_1$ | $x_2$ | $x_3$ | $x_4$ |
|---|---|---|---|---|---|---|
| $p_1$ | 0 | 0 | 0 | +1 | -1 | +1 |
| $p_2$ | 0 | 0 | +1 | 0 | 0 | -1 |
| $p_3$ | 0 | +1 | -1 | 0 | 0 | 0 |
| $p_4$ | 0 | 0 | 0 | 0 | 0 | 0 |
| $p_5$ | +1 | 0 | -1 | 0 | 0 | 0 |

| | $y_1$ | $y_2$ | $x_1$ | $x_4$ | $x_3$ | $x_2$ |
|---|---|---|---|---|---|---|
| $p_5$ | +1 | 0 | -1 | 0 | 0 | 0 |
| $p_3$ | 0 | +1 | $\mathbf{-1}$ | 0 | 0 | 0 |
| $p_2$ | 0 | 0 | +1 | $\mathbf{-1}$ | 0 | 0 |
| $p_1$ | 0 | 0 | 0 | +1 | $\mathbf{-1}$ | +1 |
| $p_4$ | 0 | 0 | 0 | 0 | 0 | 0 |

With that aim in view, the two phases of the proposed approach are:

- The first phase is a structural analysis of the large scale Petri net based on the canonical decomposition of A. L. Dulmage and N. S. Mendelsohn, which focuses on the connections between the firing counts of the unobservable transitions. This structural analysis of $W_{un}$ allows to determine a set of sub-systems, which are the support of a possible resolution. In the context of continuous systems, Appendix 1 9 illustrates the DM resolution and the relevant resolution with is a simple electrical system.

- The second phase in Section 6 is a sequential resolution based on the block triangular form proposed in the first phase.

We now analyze the incidence matrix $W_{un}$ of the UIPNs represented by a bipartite graph ($P$, $TR_{un}$) connecting the places and the unobservable transitions in the non-weighted case and perfect case. The mathematical notation of [17] [18] is adapted to the context of Petri nets. Another presentation of the DM decomposition with different examples in the non-weighted case can be found in the appendix of [11].

## 4.2 Maximum matching

Let us consider two simplified cases, which allow to present and apply the canonical decomposition of bipartite graphs.

### 4.2.1 Non-weighted case

Let us consider the *non-weighted case,* which corresponds to a boolean point of view and which has been analyzed by A. L. Dulmage and N. S. Mendelsohn [17] [18]: only the existence of non-null components in the incidence matrix $W_{un}$, is considered. So, the difference between positive and negative components in the incidence matrix $W_{un}$, is not made and the orientation of the arcs in the UIPN is not considered.

We consider the matching between the relations $P$ and the unobservable transitions $TR_{un}$ defined as follows:

**Definition 1.** *A matching $C$ is a set of pairs $(p_i, x_j)$ where:*

- *Each place $p_i$ is associated with a transition $x_j$ at the most.*
- *Each transition $x_j \in TR_{un}$ is associated with a place $p_i$ at the most.*

So, in a matching $C$, a unique transition is associated to each place and a unique place is associated to each transition.

In the following parts, we focus on maximum matching, where the number of its pairs is maximum. Different maximum matchings can be obtained but all of them have the same cardinality. In the tables, each pair of the matching is expressed by a symbol in bold as shown in the incidence matrix at the bottom of Table 2.

Note that a possible pair can be composed of a place and one of its input or output transitions. This artificial case will be modified in the following sections.

### 4.2.2 Perfect case

Let us consider an interesting class of UIPNs which presents the following features and defines the *perfect case*: this case will be the support of the following study and corresponds mainly to FCF UIPN without unobservable source transition. Contrary to the non-weighted case, the difference between positive and negative components in the incidence matrix $W_{un}$, which corresponds to the orientation of the arcs in the UIPN is now considered.

- Assumption $\mathcal{F}-1$ : the relevant incidence matrix has no null rows (each place is associated with an unobservable transition at least).

- Assumption $\mathcal{F}-2$ : each place of the UIPN presents an output unobservable transition at least.

- Assumption $\mathcal{F}-3$ : the UIPN is FCF.

- Assumption $\mathcal{F}-4$ : the UIPN is without unobservable source unobservable transitions.

Clearly, the null rows of the unobservable incidence matrix (Assumption $\mathcal{F}-1$) and places without output unobservable transitions (Assumption $\mathcal{F}-2$) cannot be exploited to build a majorant of an unobservable transition. Treated in Section 4, these features lead to specific buildings.

Under an algebraic point of view, the event numbers of all the output transitions of a place are upper-bounded if the event numbers of all the input transitions of a place are upper-bounded: in the Petri net 2, $\overline{x}_4 \in p_2^\bullet$ is upper-bounded as $\overline{x}_1 \in^\bullet p_2$ is upper-bounded. This principle based on the dependence between variables is exploited in the structural analysis. If we desire that the matching (place, transition) expresses the upper-boundedness, only the connections describing that a transition is an output transition of a place are useful in the resolution. The following result analyzes the maximum matching which is necessary in the DM decomposition.

**Theorem 4.** *The cardinalities of the maximum matching $C$ in the case of an FCF UIPN without unobservable source transition and in the relevant non-weighted case are equal. Moreover, $|C| = |TR_{un}|$.*

**Proof.**

By definition, if the UIPN is without unobservable source transition (Assumption $\mathcal{F}-4$), each unobservable transition has an input place at least. Symmetrically, each place of the UIPN presents an output unobservable transition at least (Assumption

$\mathcal{F}-2$). Let us analyze the relevant bipartite graph connecting the places and the output unobservable transitions. For Assumption $\mathcal{F}-3$, any two distinct unobservable transitions have no common input place and we are sure that each unobservable transition has an input place at least (Assumption $\mathcal{F}-4$). Consequently, each unobservable transition can be matched with one of its input place and this matching does not modify the possibilities to match any other transition as they cannot be matched with the same place. Consequently, we can always define a matching $C$ such that each unobservable transition is matched with one of its input places and $C$ satisfies $|C| = |TR_{un}|$. Moreover, this matching is maximum since there is no greater matching than $|TR_{un}|$ even if we remove the orientation of the arcs as in the non-weighted case. ■

Each transition expressing a synchronization (that is, a transition having two input places at least) can be matched with one of its input places. In an FCF UIPN, different choices are possible for these transitions contrary to the places, which have a unique output transition. So, the number of maximum matchings is $\prod_{x_i \in TR_{un}} |{}^{\bullet}x_i|$, where $\prod$ describes the product. Particularly, a unique maximum matching is obtained when no transition of the UIPN describes a synchronization.

## 4.3 Canonical DM decomposition

### 4.3.1 Non-weighted case

Under the condition that the matching is maximum, the canonical DM decomposition [17] [18] which is now presented can be applied in the non-weighted case. The structural decomposition of the table leads to a diagonal of specific block substructures based on three distinct canonical structures named Just-, Over- and Under-structures. When the matching $C$ is maximum, the studies [17] [18] prove that there is a unique partition of rows of $P$ and columns of $TR_{un}$ denoted $X$ such that $P = P^{>} \cup P^{=} \cup P^{<}$ and $X = X^{>} \cup X^{=} \cup X^{<}$ with empty intersections, which highlights three important substructures: the Over-structure $S^{>} = (P^{>}, X^{>})$, the Just-structure $S^{=} = (P^{=}, X^{=})$ and the Under-structure $S^{<} = (P^{<}, X^{<})$. Moreover, we have $|C| = |C^{>}| + |C^{=}| + |C^{<}|$ (expression $|.|$ denotes the number of pairs in the matching), where $C^{>}, C^{=}$ and $C^{<}$ satisfy the following points.

- For the Over-structure, the maximum matching $C^{>}$ satisfies $|C^{>}| = |X^{>}| < |P^{>}|$. All elements of $X^{>}$ are matched but there is at least a non-matched element in $P^{>}$.
- For the Just-structure, the maximum matching $C^{=}$ satisfies $|C^{=}| = |P^{=}| = |X^{=}|$. All elements of $P^{=}$ and $X^{=}$ are matched in the case of a Just-structure, which can be decomposed in irreducible blocks.
- For the Under-structure, the maximum matching $C^{<}$ satisfies $|C^{<}| = |P^{<}| < |X^{<}|$. All elements of $P^{<}$ are matched but there is at least a non-matched element in $X^{<}$.

Note that $|C| = |X^{>}| + |X^{=}| + |P^{<}|$.

Given a matching, an alternating path in a UIPN is a path, in which the arcs belong alternatively to the matching and not to the matching. The maximum matching in the non-weighted case allows to determine the different substructures with the following theorem transposed from [17] [18] [12] [13]. To facilitate the presentation of the results, a direction is added to the edges of the non-oriented bipartite graph. Each pair $(p_i, x_j)$

of the maximum matching $C$ is oriented from $p_i$ to $x_j$ (graphically, $p_i \xrightarrow{C} x_j$) and in the opposite direction when $(p_i, x_j) \notin C$ (graphically, $p_i \leftarrow x_j$ ).

**Theorem 5.** *Let us assume that the matching is maximum in the non-weighted case.*

- The places and transitions of an alternating path belong to the Over-structure $S^{>} = (P^{>}, X^{>})$ when this path starts from a matched place and finishes in a non-matched place.
- The places and transitions of an alternating path belong to the Under-structure $S^{<} = (P^{<}, X^{<})$ when this path starts from a non-matched transition and finishes in a matched transition.
- The Just-structure is defined by $P^{=} = P \backslash (P^{>} \cup P^{<})$ and $X^{=} = TR_{un} \backslash (X^{>} \cup X^{<})$. ■

**Example 2 continued.**

In Table 2, the null row of $W_{un}$ cannot be exploited by the analysis which focuses on the remaining rows: we take $P = \{p_1, p_2, p_3, p_5\}$. The maximum matching $C$ with $|C| = 3$, is $C = \{(p_3, x_1), (p_2, x_4), (p_1, x_3)\}$ and is represented in bold. As the matching is maximum, Theorem 5 can be applied. It gives the DM decomposition highlighted in grey and defined as follows.

- As there is an alternating path from a matched place $p_3$ to a non-matched place $p_5$ which is $p_3 \xrightarrow{C} x_1 \rightarrow p_5$, the Over-structure is $S^{>} = P^{>} \times X^{>}$ with $P^{>} = \{p_5, p_3\}$ and $X^{>} = \{x_1\}$.
- As there is an alternating path from non-matched transition $x_2$ to a matched transition $x_3$ which is $x_2 \rightarrow p_1 \xrightarrow{C} x_3$, the Under-structure is $S^{<} = P^{<} \times X^{<}$ with $P^{<} = \{\ p_1\}$ and $X^{<} = \{x_3, x_2\}$.
- The Just-structure is $S^{=} = P^{=} \times X^{=}$ with $P^{=} = \{\ p_2\}$ and $X^{=} = \{x_4\}$. ■

Moreover, the DM decomposition is not limited to the three main canonical structures as the Just-structure $S^{=}$ presents a specific block-diagonal structure where the blocks are square. Each block is composed of transitions, where each transition is connected to any transition of the substructure with a circuit composed of places. Illustrated in Example 3 below, these substructures are usually named *strongly connected* substructure in the UIPN and, *irreducible* substructure for the corresponding representation in the incidence matrix $W_{un}$. Formally, the substructure contains a directed path from to $x_i$ to $x_j$ and a directed path from $x_j$ to $x_i$ for every pair of vertices $x_i$, $x_j$. To treat the case of substructures composed of a single vertex, a fictitious self-loop of null length connecting $x_i$ to $x_i$ is assumed to be added to each vertex $x_i \in X^{=}$.

### 4.3.2 Perfect case

This section analyzes the DM decomposition in the perfect case.

**Theorem 6.**
- *The FCF UIPN without unobservable source transition presents a canonical DM decomposition of the structure $(P, TR_{un})$ limited to $S^{>}$ and $S^{=}$: $P^{<} = \phi$ and $X^{<} = \phi$.*
- *Moreover, this canonical DM decomposition is limited to $S^{=}$ with $P^{>} = \emptyset$ and $X^{>} = \emptyset$ when $|C_{max}| = |P|$.*

**Proof**

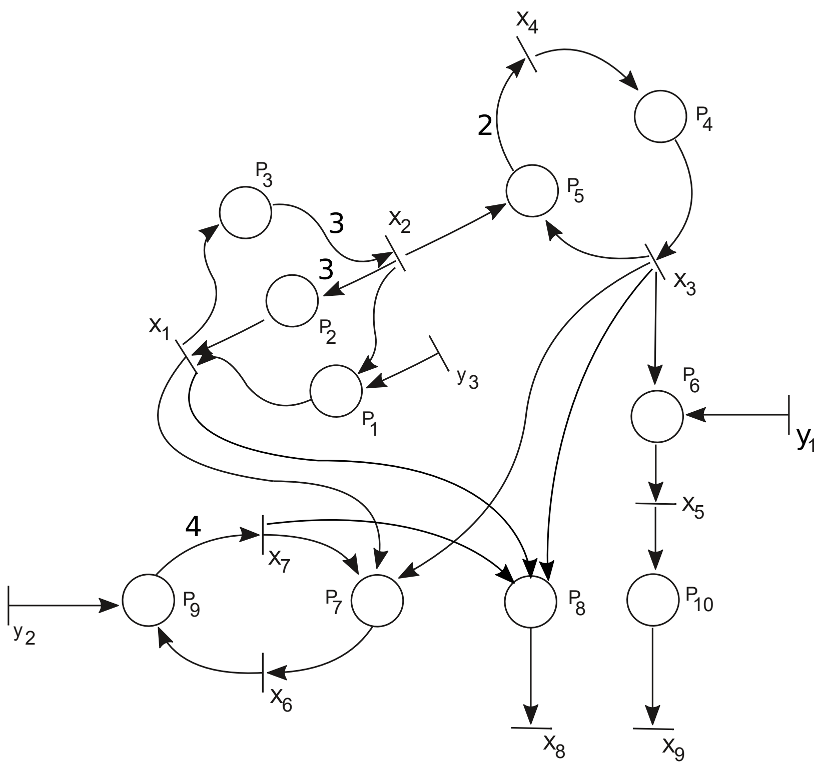


**Fig. 3** Petri net 3 of example 3; The initial marking is not represented.

For an FCF UIPN, Theorem 4 shows that the matching is maximum, which implies that the canonical DM decomposition can be applied to the considered table. As $|C_{max}| = |TR_{un}|$, no Under-structure, which needs that at least an unobservable transition is not matched is present in the structure. The canonical decomposition of place set $P$ is $P = P^{>} \cup P^{=}$ and the transition set $X$ is given by $X = X^{>} \cup X^{=}$.

Moreover, if $|C_{max}| = |P|$ , no Over-structure, which needs that at least a place is not matched is present in the structure. The structure is limited to a Just-structure, which presents a block-triangular structure of irreducible substructures. If $|C_{max}| < |P|$ , then $P^{>} \neq \emptyset$ and $X^{>} \neq \emptyset$ and the structure contains an over-structure. ■

**Example 3.**

Let us consider the Petri net 3 of Fig. 3 with an arbitrary initial marking guaranteeing the liveness. For clarity, the labels of the places and transitions have been chosen such that they follow the classification of the DM decomposition. We have: $P = \{p_1, p_2, \ldots, p_{10}\}$ with $|P| = 10$; $TR = TR_{obs} \bigcup TR_{un}$ with $TR_{obs} = \{y_1, y_2, y_3\}$ and $TR_{un} = \{x_1, x_2 \ldots, x_8, x_9\}$. All the weights of the arcs are unitary except $(W_{un})^-_{3,2} = 3, (W_{un})^+_{2,2} = 3, (W_{un})^-_{5,4} = 2$ and $(W_{un})^-_{8,7} = 4$.

The table 3 gives the connections between places and unknown variables. The maximum matching $C$ with $|C| = 9$ is $C = \{(p_2, x_1), (p_3, x_2), (p_4, x_3), (p_5, x_4), (p_6, x_5), (p_7, x_6), (p_9, x_7), (p_8, x_8), (p_{10}, x_9)\}$ and is represented in bold. As the matching is maximum, we can apply Theorem 5. So, $P = P^{>} \cup P^{=}$ and $X = X^{>} \cup X^{=}$ with:

**Table 3** Canonical decomposition of the structure of the incidence matrix of the UIPN 3 in Fig. 3 (example 3)

| | $y_1$ | $y_2$ | $y_3$ | $x_1$ | $x_2$ | $x_3$ | $x_4$ | $x_5$ | $x_6$ | $x_7$ | $x_8$ | $x_9$ |
|---|---|---|---|---|---|---|---|---|---|---|---|---|
| $p_1$ | 0 | 0 | +1 | -1 | +1 | 0 | 0 | 0 | 0 | 0 | 0 | 0 |
| $p_2$ | 0 | 0 | 0 | **−1** | +3 | 0 | 0 | 0 | 0 | 0 | 0 | 0 |
| $p_3$ | 0 | 0 | 0 | +1 | **−3** | 0 | 0 | 0 | 0 | 0 | 0 | 0 |
| $p_4$ | 0 | 0 | 0 | 0 | 0 | **−1** | +1 | 0 | 0 | 0 | 0 | 0 |
| $p_5$ | 0 | 0 | 0 | 0 | +1 | +1 | **−2** | 0 | 0 | 0 | 0 | 0 |
| $p_6$ | +1 | 0 | 0 | 0 | 0 | +1 | 0 | **−1** | 0 | 0 | 0 | 0 |
| $p_7$ | 0 | 0 | 0 | +1 | 0 | +1 | 0 | 0 | **−1** | +1 | 0 | 0 |
| $p_8$ | 0 | 0 | 0 | +1 | 0 | +1 | 0 | 0 | 0 | +1 | **−1** | 0 |
| $p_9$ | 0 | +1 | 0 | 0 | 0 | 0 | 0 | 0 | +1 | **−4** | 0 | 0 |
| $p_{10}$ | 0 | 0 | 0 | 0 | 0 | 0 | 0 | +1 | 0 | 0 | 0 | **−1** |

- The Over-structure is $P^{>} = \{p_1, p_2, p_3\}$ and $X^{>} = \{x_1, x_2\}$.
- The Just-structure is $P^{=} = \{ p_4, p_5, p_6, p_7, p_8, p_9, p_{10}\}$ and $X^{=} = \{x_3, x_4, x_5, x_6, x_7, x_8, x_9\}$.

Highlighted in grey, the Over-structure is $S_1^{>} = \{p_1, p_2, p_3\} \times \{x_1, x_2\}$ and the irreducible substructures of the Just-structure are $S_2^{=} = \{p_4, p_5\} \times \{x_3, x_4\}$, $S_3^{=} = \{p_6\} \times \{x_5\}$, $S_4^{=} = \{ p_7, p_8, p_9, p_{10}\} \times \{x_6, x_7, x_8\}$ and $S_5^{=} = \{p_{10}\} \times \{x_9\}$.

■

# 5 DM decomposition for general UIPNs

The objective of this part is to generalize the analysis of Section 4 to any Petri net by building an associated Petri net presenting the assumptions from $\mathcal{F}{-}1$ to $\mathcal{F}{-}4$. We below show that the following main treatments can always be made:

- Preliminary simplification (Assumptions $\mathcal{F}{-}1, \mathcal{F}{-}2$ and building 1)
- The building of an FCF UIPN (Assumption $\mathcal{F}{-}3$ and building 2).
- The building of a Petri net without unobservable source transitions (Assumption $\mathcal{F}{-}4$ and building 3).

## 5.1 Preliminary simplification (Building 1)

In the analysis of the UIPN, the null rows of the unobservable incidence matrix cannot be exploited and can be removed: $(W_{un})_{l,..} \neq 0$ for any place $p_l$ (Assumption $\mathcal{F}{-}1$). In Example 2, the null row relevant to $p_4$ in Table 2 illustrates this point.

Moreover, even if the UIPN is FCF, a possible case is that a place $p_l$ does not have an output unobservable transition (formally, $|p_l^{\bullet} \cap TR_{un}| = 0$ or $(W_{un})^{-}_{l,..} = 0$). Consequently, this place cannot be exploited to build a majorant of an unobservable transition. The relevant unnecessary row in $W_{un}$ must be removed. In other words, all the rows of $W_{un}$ relevant to a place $p_l$ with $|p_l^{\bullet} \cap TR_{un}| \neq 0$ (so, $W_{un})^{-}_{l,.i} \neq 0$) must be kept. As the withdraw of a place can create a null column in $W_{un}$, the relevant unobservable transition are not upper-bounded and the column can be removed from the table. A consequence is that that each place in the simplified Petri net presents an output unobservable transition at least (Assumption $\mathcal{F}-2$).

**Example 3 continued.**

Let us consider the Petri net 3 in Fig. 3 (example 3) but we add a place $p_0$, which presents two entering unobservable transitions $x_1, x_2$ and an entering observable transition $y_2$. This place $p_0$ cannot be exploited to build a majorant and can be removed. ■

To limit the analysis to the useful part of the UIPN, Assumptions $\mathcal{F}-1$ and $\mathcal{F}-2$ are taken below. To facilitate the writing and alleviate the notation, we below keep the same notation for the reduced set of places ($P$), the reduced set of unobservable transitions ($TR_{un}$) and the different incidence matrices $W$, $W_{obs}$ and $W_{un}$ as they are defined by the context. This abuse of notation is made at each modification of the Petri net below.

## 5.2 Generalization to non-FCF UIPN (building 2)

The following theorem shows that we can generalize the previous approach to UIPNs, which are not FCF. The technique is to build an FCF UIPN with a simplification of the valuations.

**Theorem 7.** *The propagation of the upper-boundedness of the firing numbers of the unobservable transitions is solely forward with respect to the arc direction of the Petri net. Moreover, for a place $p_l$ with $|p_l^\bullet \cap TR_{un}| \neq 0$ (equivalently, $(W_{un})^-_{l,.} \neq 0$), the analysis of the upper-boundedness of the firing numbers for (5) relaxed over $\mathbb{R}$ and the following system*

$$\overline{x}_i \leq b^{<k>} + (W_{un})^+_{l,.}.\overline{x} \text{ for any } x_i \in p_l^\bullet \cap TR_{un}, \tag{6}$$

where $\overline{x}$ is over $\mathbb{R}$ are equivalent.

**Proof.**

Let us analyze a place $p_l$ with $|p_l^\bullet \cap TR_{un}| \neq 1$ and the different relations.

- Relation (5) ( $-W_{un}.\overline{x}^{<0>\to<k>} \leq b^{<k>}$) relaxed over $\mathbb{R}$ is rewritten under the more convenient form $(W_{un})^-_{l,.}.\overline{x} \leq b^{<k>} + (W_{un})^+_{l,.}.\overline{x}$ with $b^{<k>} = M^{<1>} + W_{obs} \cdot \overline{y}^{<0>\to<k-1>} - W^-_{obs}.\overline{y}^{<k>}$. We assume that all $\overline{x}_j$ for $x_j \in {}^\bullet p_l \cap TR_{un}$ are upper-bounded in (5) and (6).

Consequently, $b^{<k>} + (W_{un})^+_{l,.}.\overline{x}$ in (5) is upper-bounded as $(W_{un})^+_{l,.} \geq 0$. The same conclusion holds for $b^{<k>} + (W_{un})^+_{l,.}.\overline{x}$ as $(W_{un})^+_{l,.} \geq 0$.

- For (5), $(W_{un})^-_{l,.}.\overline{x}$ for a given place $p_l$ is upper-bounded by a bound, which implies that all terms $\overline{x}_i$ for $x_i \in p_l^\bullet \cap TR_{un}$ satisfying $(W_{un})^-_{l,i} > 0$ are also upper-bounded since $(W_{un})^-_{l,i} = 0$ for $x_i \notin p_l^\bullet \cap TR_{un}$. Note that the converse cannot be said: if all terms $\overline{x}_i$ for $x_i \in p_l^\bullet \cap TR_{un}$ are upper-bounded, we cannot conclude from the analysis of this place $p_l$ that some $\overline{x}_j$ for $x_j \in {}^\bullet p_l \cap TR_{un}$ are upper-bounded by a finite value. Consequently, the propagation of the upper-boundedness is uniquely forward.

- For (6), we can immediately deduce that each term $\overline{x}_i$ for $x_i \in p_l^\bullet \cap TR_{un}$ is upper-bounded, which implies that $(W_{un})^-_{l,.}.\overline{x}$ is also upper-bounded.

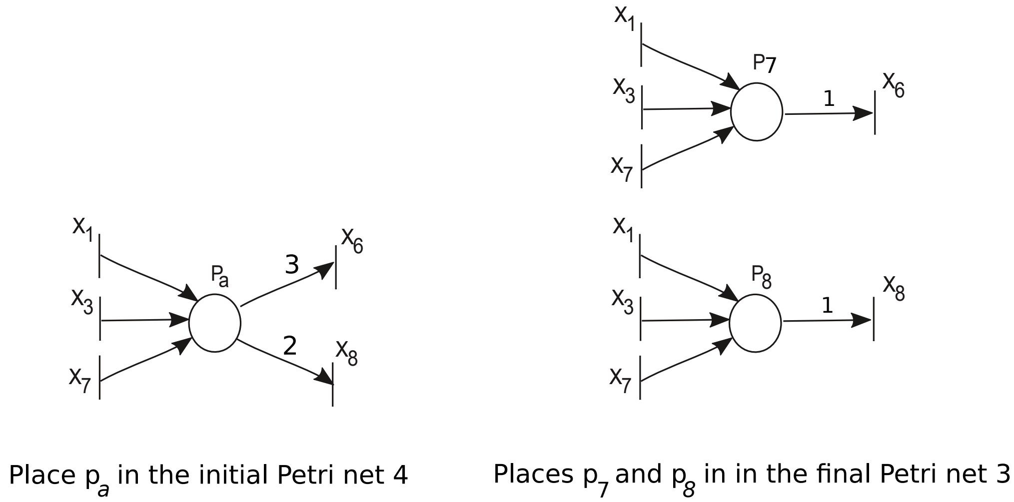


**Fig. 4** Place $p_a$ is replaced by $p_7$ and $p_8$ in Fig. 3

Therefore, the same conclusions for (5) and (6) for a place $p_l$ can be made. The generalization to a system of relations relevant to a set of places, which only add constraints cannot limit the above reasoning and the analysis of the upper-boundedness are equivalent. ■

Note that if there are some $x_j \in {}^\bullet p_l \cap TR_{un}$, which are not upper-bounded, we cannot conclude from the analysis of this place $p_l$ that $(W_{un})^-_{l,.}.\overline{x}$ is upper-bounded by a finite bound and that all terms $\overline{x}_i$ for $i \in p_l^\bullet \cap TR_{un}$ are upper-bounded for (5) and the set of $|p_l^\bullet \cap TR_{un}|$ relations (6). This case is considered in Section 5.3.

Another remark is that the two systems (5) relaxed over $\mathbb{R}$ and (6) are not algebraically equivalent (as we focus on the analysis of the upper-boundedness of the firing numbers). Particularly, the valuations of the outgoing arcs become unitary in (6) and the deduced Petri net.

Therefore, the building of an FCF UIPN will facilitate the determination of the maximum matching in the structural analysis. This construction replaces each place with $|p_l^\bullet \cap TR_{un}| \neq 0$ by a set of $|p_l^\bullet \cap TR_{un}|$ places.

**Construction of an FCF UIPN and its new incidence matrix $W'$(Building 2)**

For each outgoing arc going from a place $p_l$ with $|p_l^\bullet \cap TR_{un}| \geq 2$ (so, $W_{un})^-_{l,.i} \neq 0$) to a transition $x_i \in p_l^\bullet \cap TR_{un}$, build a row $l'$ in $W'$ such that
$(W'_{obs})^+_{l',.} = (W_{obs})^+_{l,.}$, $(W'_{obs})^-_{l',.} = (W_{obs})^-_{l,.}$ (no modification) and
$(W'_{un})^+_{l',.} = (W_{un})^+_{l,.}$, $(W'_{un})^-_{l',.} = 0$ except $(W'_{un})^-_{l',i} = 1$ (the UIPN is modified).
The relevant new places keep the initial marking of the initial place $p_l$.
■

**Example 3 continued.**

Let us consider the Petri net 3 in Fig. 3 (example 3) but places $p_7$ and $p_8$ are substituted by a place $p_a$ presenting the same input unobservable transitions $x_1$, $x_3$,

$x_7$ but the two output unobservable transitions $x_6$, $x_8$ (Fig. 4). The relevant Petri net is denoted Petri net 4 and the substructure corresponding to $S_4^{=}$ is represented in table 4. This substructure is not square and not irreducible a fortiori.

**Table 4** Structure of $S_4^{=}$ for Petri net 4 in Fig. 4

| | $y_1$ | $y_2$ | $y_3$ | $x_1$ | $x_2$ | $x_3$ | $x_4$ | $x_5$ | $x_6$ | $x_7$ | $x_8$ | $x_9$ |
|---|---|---|---|---|---|---|---|---|---|---|---|---|
| $p_a$ | 0 | 0 | 0 | +1 | 0 | +1 | 0 | 0 | -3 | +1 | -2 | 0 |
| $p_9$ | 0 | +1 | 0 | 0 | 0 | 0 | 0 | 0 | +1 | -4 | 0 | 0 |

So, the UIPN is not FCF. Place $p_a$ is described by relation $p_a : 3.\overline{x}_6 + 2.\overline{x}_8 \leq M_a^{init} + \overline{x}_1 + \overline{x}_3 + \overline{x}_7$

The previous theorem shows that the analysis of the upper-boundedness can be made with the Petri net in Fig. 3, where $p_a$ is replaced by places $p_7$ and $p_8$.

$p_7 : \overline{x}_6 \leq M_a^{init} + \overline{x}_1 + \overline{x}_3 + \overline{x}_7$

$p_8 : \overline{x}_8 \leq M_a^{init} + \overline{x}_1 + \overline{x}_3 + \overline{x}_7$ ■

Assumptions $\mathcal{F}-1$, $\mathcal{F}-2$ and $\mathcal{F}-3$, which are obtained with the buildings 1 and 2 for any Petri net, are assumed in the sequel.

## 5.3 FCF UIPNs with unobservable source transitions (building 3)

By definition, an unobservable source transition is not the output transition of a place. It cannot be upper-bounded and be used to limit other transitions. Consequently, if a unobservable source transition is the input of a place (even if other input transitions exist), the relevant relation does not bring an upper bound on the output transitions and this place (and the relevant arcs) must be removed. This manipulation can create some unobservable source transitions and the same reasoning must be repeated until the UIPN has no unobservable source transition. A direct consequence of the elimination is the application of Theorem 6 : the FCF UIPN after elimination of the unobservable source transitions presents a canonical DM decomposition.

**Elimination of the substructure connected to the unobservable source transitions (Building 3)**

While there is a column $j$ of the incidence matrix $(W_{un})$ containing only non-negative components $((W_{un})_{.,,j} \geq 0)$ (this column corresponds to a source transition $x_j$),

- For each $i$ such that $(W_{un})_{i,j} > 0$, remove the row $i$ of the incidence matrix $(W_{un})$ : the output places of the source transition $x_j$ with their upstream and downstream arcs are removed.

- Remove column $j$.

End-while

Remove all the remaining null columns $j$ of $(W_{un})$ $((W_{un})_{.,j} = 0)$. ■

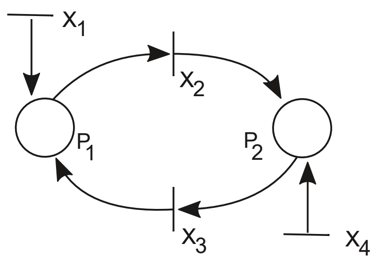


**Fig. 5** Petri net 5 (example 5)

**Example 4.** Let $W_{un} = \begin{pmatrix} 1 & 1 & -1 & 0 \\ 0 & 0 & 1 & -1 \\ 0 & -1 & 0 & 0 \end{pmatrix}$ describing an FCF UIPN. As $x_1$ is a unobservable source transition, the first column and the row of $p_1$ are removed. This implies that $x_3$ is a new unobservable source transition: the third column of $W_{un}$ and the row of $p_2$ are removed. The unique useful row of $p_3$ is kept. The last column, which is null is removed. ■

**Example 5.**

Let $W_{un} = \begin{pmatrix} 0 & -1 & 1 & 1 \\ 1 & 1 & -1 & 0 \end{pmatrix}$ describing the UIPN of the Petri net 5 of Fig. 5, which is FCF. The rows of $W_{un}$ correspond to places $p_{11}$ and $p_{12}$. The columns correspond respectively to transitions $x_8$, $x_{10}$, $x_{11}$, $x_{12}$. As $x_{12}$ is a unobservable source transition, the last column and the row of $p_1$ are removed. This implies that $x_{10}$ is a new unobservable source transition: the second column of $W_{un}$ and the row of $p_2$ are removed. ■

Therefore, the algorithm allows to build an FCF UIPN without unobservable source transitions and guarantees that the canonical DM decomposition of the structure limited to $S^{>}$ and $S^{=}$ can always be obtained.

**Theorem 8.** *Let consider a UIPN satisfying Assumptions $\mathcal{F}-1$, $\mathcal{F}-2$ and $\mathcal{F}-3$. The maximum matching satisfies $|C| = |TR_{un} \backslash UST|$, where $UST$ is the set of unobservable source transitions.*

**Proof.**

As the unobservable source transitions cannot be used in the matching as they are not output transitions of the places, they can be disregarded without affecting the matching. Let $UST$ be the set of unobservable source transitions. So, the matching can be made between the set of places $P$ and the remaining unobservable transitions $TR_{un} \backslash UST$. In some way, Assumption $\mathcal{F}-4$ is satisfied and this situation corresponds to the features of Theorem 4, which can be applied: the maximum matching satisfies $|C| = |TR_{un} \backslash UST|$.
■

Let us note that if a fictive place is associated with each unobservable source transition, this source transition disappears. In that case, Theorems 4 and 6 can be applied and a DM decomposition without under-structure is obtained. Particularly, a matching between this fictive place and the source transition is obtained. Now, if we analyze the elimination technique, the building 3 corresponds to the construction of alternating paths starting from each unobservable source transition, which is non-matched. Therefore, the building 3 is now interpret not as a technique to eliminate an undesirable part, but to determine a specific substructure. In other words, the building 3 is not used to modify the Petri net but to analyze its internal structure.

**Theorem 9.** *Let consider a UIPN satisfying Assumptions $\mathcal{F}-1$, $\mathcal{F}-2$ and $\mathcal{F}-3$.*

- The cardinalities of the maximum matching $C$ in the case of an FCF UIPNs with unobservable source transition and in the relevant non-weighted case are equal.
- The places and transitions of an alternating path belong to the Over-structure $S^{>} = (P^{>}, X^{>})$ when this path starts from a matched place and finishes in a non-matched place.
- The places and transitions of an alternating path belong to the Under-structure $S^{<} = (P^{<}, X^{<})$ when this path starts from a unobservable source transition and finishes in a matched transition.
- The Just-structure is defined by $P^{=} = P \backslash (P^{>} \cup P^{<})$ and $X^{=} = TR_{un} \backslash (X^{>} \cup X^{<})$. ■

**Proof.**

The previous theorem 8 says that the maximum matching satisfies $|C| = |TR_{un} \backslash UST|$ and that all the transitions of $TR_{un} \backslash UST$ are matched. We can consider the alternating paths based on this matching. Particularly, the analysis of building 3 shows that the elimination technique corresponds to the construction of alternating paths starting from each unobservable source transition, which is non-matched. So, these alternating paths define the Under-structure $S^{<} = (P^{<}, X^{<})$ with $|C^{<}| = |P^{<}|$, which can be removed: consequently, the relevant UIPN is without unobservable source transition (Assumption $\mathcal{F}-4$) and the assumptions of Theorems 4 and 6 are fulfilled: the cardinalities of the maximum matching $C'$ in the case of an FCF UIPN defined by $(P \backslash P^{<}, TR_{un} \backslash X^{<})$ and in the relevant non-weighted case are equal. Also, $|C'| = |TR_{un} \backslash X^{<}|$, the DM decomposition of the structure is limited to $S^{>}$ and $S^{=}$ and $|C'| = |X^{>}| + |X^{=}|$. Finally, $|C| = |C'| + |C^{<}| = |X^{>}| + |X^{=}| + |P^{<}|$, which corresponds to the non-weighted case.

■

**Example 3 continued.**

We now desire analyze a Petri net denoted as Petri net 6, which is the concatenation of the Petri net 4 (this variant of the Petri net 3 is presented in Section 5.2) and the Petri net 5 of Fig. 5. In Petri net 6, places $p_7$ and $p_8$ are substituted by a place $p_a$ ( Section 5.2 and Fig. 4). Moreover, the following modification of notation is made: now the places $p_1$ and $p_2$ of Fig. 5 are denoted $p_{11}$ and $p_{12}$ and transitions $x_1$, $x_2$, $x_3$, $x_4$ are denoted $x_8$, $x_{11}$, $x_{10}$, $x_{12}$. For simplicity sake, the other notations are kept. The table describing $p_{11}$ and $p_{12}$ is table 5.

Therefore, the Petri net 6, which represents the general case does not satisfy Assumption $\mathcal{F}-3$ as the UIPN is not FCF (place $p_a$). Moreover, Assumption $\mathcal{F}-4$ is not satisfied as the Petri net 6 presents a unobservable source transition $x_{12}$.

As the Petri net 6 cannot directly be treated, an associated Petri net denoted Petri net 7 must be established. To obtain an FCF UIPN, we can apply the building 2, that is, the development of place $p_a$ with provides the places $p_7$ and $p_8$ as explained in

**Table 5** Table deduced from the Petri net 5 of Fig. 5 with new notations

| | $y_1$ | $y_2$ | $y_3$ | $x_1$ | $x_2$ | $x_3$ | $x_4$ | $x_5$ | $x_6$ | $x_7$ | $x_8$ | $x_9$ | $x_{10}$ | $x_{11}$ | $x_{12}$ |
|---|---|---|---|---|---|---|---|---|---|---|---|---|---|---|---|
| $p_{11}$ | 0 | 0 | 0 | 0 | 0 | 0 | 0 | 0 | 0 | 0 | 0 | 0 | $\mathbf{-1}$ | $+1$ | $+1$ |
| $p_{12}$ | 0 | 0 | 0 | 0 | 0 | 0 | 0 | 0 | 0 | 0 | $+1$ | 0 | $+1$ | $\mathbf{-1}$ | 0 |

Section 5.2 (see Fig. 4). The table of the associated UIPN is the concatenation of table 3 (Petri net 3 of Fig. 3) and table 5 relevant to the Petri net 5 of Fig. 5 with the new places and unobservable transitions. The DM decomposition is deduced from theorem 9. The same substructures already obtained in Section 4.2.2 and presented in table 3 are kept while the under-structure $S^{<}$ denoted as the substructure $S_6$ is deduced with Building 3 (example 5 and Fig. 5) and is added. Therefore, the substructures of the UIPN of Petri net 7 are $S_1^{>} = \{p_1, p_2, p_3\} \times \{x_1, x_2\}$, $S_2^{=} = \{p_4, p_5\} \times \{x_3, x_4\}$, $S_3^{=} = \{p_6\} \times \{x_5\}$, $S_4^{=} = \{\ p_7,\ p_8,\ p_9\} \times \{x_6, x_7, x_8\}$, $S_5^{=} = \{\ p_{10}\} \times \{x_9\}$ and $S^{<} = S_6^{<} = \{p_{11},\ p_{12}\} \times \{x_{10}, x_{11}, x_{12}\}$. The substructures of the UIPN of Petri net 6 are similar but $S_4^{=}$ is replaced by $\{\ p_a,\ p_9\} \times \{x_6, x_7, x_8\}$. ■

### 5.4 Numerical analysis of the off-line decomposition

In Sections 4 and 5, the structural analysis has shown that the DM decomposition can be applied to the UIPNs satisfying Assumptions $\mathcal{F}-1$, $\mathcal{F}-2$ and $\mathcal{F}-3$, which can be obtained with the buildings 1 and 2 for any Petri net (the building 3 is not necessary as said above). As these buildings are simple transformations (elimination of null rows, construction of FCF places,...), the relevant execution time is negligible with respect to the DM decomposition which must be added. This last one can be obtained with the function *dmperm()* of the software Matlab and GNU Octave which also determines the maximum matching (function *matchpairs()*). The function *dmperm()* is really efficient as the execution time is less than 0.1 seconds for a (1000×1000) matrix which corresponds to a Petri net with 1000 places and 1000 unobservable transitions. As the time complexity of the DM decomposition is dominated by the cost of computing an initial maximum matching [27], the global time complexity of the structural analysis is the complexity of the maximum cardinality matching which presents a polynomial time: the global time complexity in the worst case is $O(n^3)$ if an improvement of the Hungarian method made by Edmonds and Karp is taken ($O(n^{2.5})$ for the Hopcroft-Karp algorithm). To summarize, the execution time of the structural analysis is negligible and cannot represent a limitation of this phase, which moreover, is made off-line.

## 6 On-line sequential resolution based on the block triangular form

The result of the *off-line* decomposition of Section 5 based on Section 4 is a block triangular structure, where the top right corner contains null elements only. For each block, a rank can be numbered from the upper left corner (which can be the overstructure if it exists) to the lower right corner of the table (which can be the understructure if it exists). Showing the practical interest of the approach, the following theorem analyzes the propagation of the resolution, as in Theorem 7, but for the blocks.

**Theorem 10.** *The propagation of the upper-boundedness through the blocks is forward with respect to the rank of the blocks of the DM decomposition. The block resolution starts from the first block.*

**Proof.**

As we consider an FCF UIPN, each row contains a unique negative component ($-1$ in the examples) which belongs to a block $S^{>}$, or an irreducible block of $S^{=}$, or a block $S^{<}$. Consequently, all other elements of each row are nonnegative (0 or a a positive value). Particularly, the part outside the blocks in the bottom left corner of the table contains only nonnegative values and each positive value represents an (oriented) arc from a variable to a place, which gives the orientation of the resolution: this positive component expresses a direct dependence from the block, where the unobservable transition is an output (deduced from the column of the positive component, this block is upstream in the DM decomposition) to the block, where this place has the relevant input transition (deduced from the row of the positive component). So, the propagation of the block resolution is uniquely forward from the upstream blocks to the downstream blocks. This dependence between the blocks, which is represented by an acyclic dependence graph in Fig. 6 is consistent with the increasing order of the rank and suggests the order of resolution, which is sequential. For each block, the resolution must only consider the relevant places and transitions of all the upstream blocks and the treatment of a set of blocks is not necessary. As the first block has no dependence with another block (no component at the left of this block), the resolution is autonomous and can be made. Knowing the values relevant to the first block, the resolution of the second block, which becomes autonomous can be made. The reasoning is similar for the other blocks. ∎

## 6.1 Example 3 continued

The concatenation of table 3 (Petri net 3 of Fig. 3) and table 5 (Petri net 5 of Fig. 5) is relevant to Petri net 7 which is the associated UIPN of Petri net 6. The incidence matrix of this UIPN presents a block-triangular form obtained with the DM decomposition which suggests a potential resolution, where a series of subsystems presented below are solved in the increasing order as shown in Fig. 6. Now, we consider the structure of the Petri net 6 which has almost the same block-triangular form except the fourth structure $S_4^{=}$.

$W_{un,1} = \begin{pmatrix} -1 & 1 \\ -1 & 3 \\ 1 & -3 \end{pmatrix}$ for $S_1$, $W_{un,2} = \begin{pmatrix} -1 & 1 \\ 1 & -2 \end{pmatrix}$ for $S_2$, $W_{un,3} = (-1)$ for $S_3$, $W_{un,4} = \begin{pmatrix} -3 & 1 & -2 \\ 1 & -4 & 0 \end{pmatrix}$ for $S_4$ (described in Section 5.2 with table 4), $W_{un,5} = (-1)$

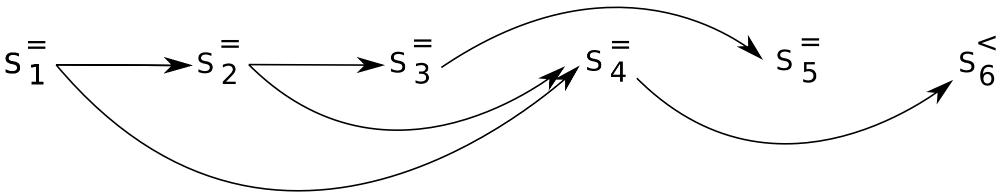


**Fig. 6** Dependences in the DM decomposition of the associated UIPN of Petri net 6.

for $S_5$, and $W_{un,6} = \begin{pmatrix} -1 & 1 & 1 \\ 1 & -1 & 0 \end{pmatrix}$ for the last substructure (described in Section 5.3 with table 5).

For simplicity, we consider the two first substructures. A possible simulation is $\begin{pmatrix} M_1^{init} \\ M_2^{init} \\ M_3^{init} \\ M_4^{init} \\ M_5^{init} \end{pmatrix} = \begin{pmatrix} 3 \\ 3 \\ 0 \\ 1 \\ 0 \end{pmatrix} \overset{x_3}{\rightarrow} \begin{pmatrix} 3 \\ 3 \\ 0 \\ 0 \\ 1 \end{pmatrix} \overset{x_1 x_1 x_1}{\rightarrow} \begin{pmatrix} 0 \\ 0 \\ 3 \\ 0 \\ 1 \end{pmatrix} \overset{x_2}{\rightarrow} \begin{pmatrix} 1 \\ 3 \\ 0 \\ 0 \\ 2 \end{pmatrix} \overset{x_1}{\rightarrow} \begin{pmatrix} 0 \\ 2 \\ 0 \\ 0 \\ 2 \end{pmatrix} \overset{x_4}{\rightarrow} \begin{pmatrix} 0 \\ 2 \\ 0 \\ 1 \\ 0 \end{pmatrix} \overset{y_3}{\rightarrow} \begin{pmatrix} 1 \\ 2 \\ 0 \\ 1 \\ 0 \end{pmatrix}$.

So, the sequence of simulation is $\sigma = x_3 x_1 x_1 x_1 x_2 x_1 x_4 y_3$. Assuming that the sequence is unknown, we desire to estimate a relevant guaranteed horizon $h_g^{<1>}$, knowing the initial marking and the firing count of $y_3$. Let us show that a direct resolution by hand of (5) relaxed over $\mathbb{R}$ can be made: the execution time is clearly negligible. For the first substructure $S_1$, the relations are $\overline{x}_1 \leq \overline{x}_2 + M_1^{init} + y_3$, $\overline{x}_1 \leq 3.\overline{x}_2 + M_2^{init}$ and $3.\overline{x}_2 \leq \overline{x}_1 + M_3^{init}$. We deduce $3.\overline{x}_2 - M_3^{init} \leq \overline{x}_1 \leq \min(\overline{x}_2 + M_1^{init} + y_3, 3.\overline{x}_2 + M_2^{init})$ , $2.\overline{x}_2 \leq M_1^{init} + M_3^{init} + y_3$ and $0 \leq M_2^{init} + M_3^{init}$. So, we can make a simple estimation with $\overline{x}_2 \leq 3/2$ and $\overline{x}_1 \leq 4$ and the greatest estimate over $\mathbb{R}$ are $\overline{x}_2 = 3/2$ and $\overline{x}_1 = 4$. So, $\nabla_{\max}^{<1>} = \lfloor 4 + 3/2 \rfloor = 5$ for $S_1$ : the number of firings of transitions $x_1$ and $x_2$ is lower than or equal to 5, which is consistent with $\sigma$. If we remove Assumption $AS - 6$ , a shorter sequence, where the three first firings of $x_1$ in $\sigma$ are simultaneous is also possible. For the second substructure $S_2$, the relations are $\overline{x}_3 \leq \overline{x}_4 + M_4^{init}$ and $2.\overline{x}_4 \leq \overline{x}_2 + \overline{x}_3 + M_5^{init}$, which gives $\overline{x}_3 \leq \overline{x}_2 + 2.M_4^{init} + M_5^{init}$ and $\overline{x}_4 \leq \overline{x}_2 + M_4^{init} + M_5^{init}$: the relevant greatest estimates can be deduced from the greatest estimate of $\overline{x}_2 = 3/2$ computed with the first substructure. We obtain $\overline{x}_3 \leq 7/2$ and $\overline{x}_4 \leq 5/2$. So, $\nabla_{\max}^{<1>} = \lfloor 7/2 + 5/2 \rfloor = 6$ for $S_2$: the number of firings of transitions $x_3$ and $x_4$ is lower than or equal to 6, which is consistent with $\sigma$. So, a guaranteed horizon is $h_g^{<1>} = \lfloor 4 + 3/2 + 7/2 + 5/2 \rfloor + 1 = \lfloor 25/2 \rfloor = 12$ for $S_1$ and $S_2$, which is coherent with the sequence of simulation $\sigma$, which represents 8 firings. The computation of the remaining unknown firing counts based on substructures $S_3, S_4, \ldots$ follows the same reasoning. ■

### 6.2 Example 6.

Let us make a numerical analysis of the on-line resolution based on more complex problems and show that the proposed approach can be applied to another estimation problem described in [3] for a classical automated manufacturing system described in Section VII.A of [25] and Section V of [11] (these papers are easily accessible). This system is a large scale system recognized to be significant in the literature since slight variations of it have already been considered by different authors. The relevant Petri net has 38 places and 26 transitions which are composed of 12 observable transitions and 14 unobservable transitions (Fig. 3 page 979 in [25], Fig. 2 in [11]). As the incidence matrix of the unobservable induced subnet is large ($38 \times 14$) but sparse, an application of the DM decomposition gives a reorganization of the rows and columns providing a clearer view under a block-triangular form presented in [11]. Let us apply the structural approach to the estimation approach presented in [3] which is limited to a unique basis marking and a maximization of an unitary criterion (as shown in [2] [3], the criterion can be adapted to detect transition firings and to make fault detection).

Let us consider the simulation given in Table I of [25] and the case of 15 observations. The scripts build the necessary matrices which increase with the horizon fixed by the number of observations. A system of 608 inequalities with 224 variables for the complete system is obtained while the greatest subsystem given by the structural approach only presents 128 inequalities with 64 variables: this reduction of size represents an improvement of the necessary memory. Using the software Scilab with the library FOT, the computations using ILP are carried out on a PC Intel(R) Core(TM) 1.90GHz 2.11 GHz. The Integer Linear Programming problems are solved with the function *fot_intlinprog()*. The relevant CPU time (the function *timer()* provides this datum) of the script execution is 0.601 seconds for the complete system and 0.148 seconds for the sequential resolution based on the structural approach (a mean value is calculated on ten executions). The decrease of the execution time shows a second improvement despite that the decomposition has only built five subsystems. Now, a similar improvement is obtained if the problems are relaxed over the real numbers: the CPU time averages are 0.605 seconds and 0.037 seconds respectively when *fot_linprog()* is used.

## 7 Efficiency of the on-line phase and limitations of the approach

Generally speaking, this approach is well-adapted to large scale systems where the induced unobservable incidence matrix is sparse and can be decomposed into a set of blocks provided by the DM decomposition. However, the following analysis suggests that the contribution can be reduced when the number of blocks is limited. Another factor is the complexity of the chosen algorithm applied in the on-line estimation. To analyze the effects of these factors, we consider that the DM decomposition of the induced unobservable incidence matrix has lead to a simple bloc diagonal structure composed of $s$ square substructures which have the same size: even if this assumption is rather strong, it allows to approximate the general effects. We also assume that the complexity of the used algorithm is polynomial with $O(n^q)$ in the worst case where $q$ is a natural number. So, the execution time presents the asymptotic form $\alpha.n^q.\Delta$ where $\Delta$ is the execution time of an elementary operation and $\alpha$ is a constant when $n$ is sufficiently large. As the dimensions of each substructure is $(n/s\mathrm{x}n/s)$, the execution time is asymptotically $s.\alpha.(n/s)^q.\Delta = (\alpha.n^q.\Delta)/s^{q-1}$ for the complete system, the substitution coming from the connections between the blocks being negligible. So, the asymptotic form of the execution time in the worst case is divided by $s^{q-1}$ for $n$ sufficiently large and $q \geq 2$. To sum up, this asymptotic form which provides a guaranteed upper bound on the algorithm's performance is improved even if the improvement of this bound can be weak when the algorithm is efficient and the number of blocks limited as in Example 6 (assuming that the complexity of the used algorithm is $O(n^2)$, the asymptotic ratio $s^{q-1}$ is equal to 5 for $s = 5$ and $q = 2$). This analysis is coherent with the papers [34] [35] [36] even if the considered structure is a variant of the block triangular structure where the blocks are clans based on a relation of nearness: an improvement is deduced for polynomial algorithms while solving a few systems with lesser size under the condition of exponential complexity allows and exponential speedup of computation.

# 8 Conclusion and perspectives

In this paper, we have considered the on-line estimation of maximum sequence length in Partially Observable Petri Nets, which allows to consider any criterion. As continuous models modelled by differential-algebraic equations, the class of Petri nets presents a computational causal direction for each place: Theorem 7 shows that the propagation of the upper-boundedness of the firing numbers of the unobservable transitions is solely forward through the UIPN with respect to the arc orientation of the Petri net. This property allows to exploit the structural analysis based on the DM decomposition presented in Section 4, which is generalized in Section 5. As a condition of this canonical decomposition is the maximum matching as in the non-weighted case, we have shown that a treatment is possible after the building of a simplified FCF unobservable subnet. The dependence graph clearly describes the connections between the blocks and suggests a sequential resolution, which allows to avoid the treatment of the large scale system in one single stage.

The different algorithms of structural analysis in the off-line phase correspond to efficient manipulations in classical path theory [28]. For the on-line phase, Section 7 suggests a performance improvement brought by the proposed approach which depends on some factors as the number of blocks (which must be sufficient) and the efficiency of the algorithms (which can minimize the improvement). A pertinent situation is the case of combinatorics problems leading to exponential complexity: this situation can appear when the estimation tries to provide all the solution set of the trajectories or the markings; the verification of protocols is another application [34] [35] [36]. A perspective is the development of tests considering the different parameters defining the Petri nets (density, number and dimension of the blocks,... ) and the used algorithms [20]. Note that other types of decompositions as the clan decomposition or a variant of the DM decomposition [11] can be tried and possibly exploited before the on-line stage. Other perspectives can be the adaptation of the Dulmage-Mendelsohn decomposition to various complex problems of estimation and control for large scale systems. The extension of the state estimation to models containing discrete event subsystems but also continuous subsystems is a natural perspective.

# 9 Appendix 1 Continuous systems: a simple electrical system

Let us illustrate the main concepts of the DM decomposition with a simple electrical circuit model.

**Example 7.**

Four resistors are connected with a voltage source as shown in Fig. 7. Symbols $V$

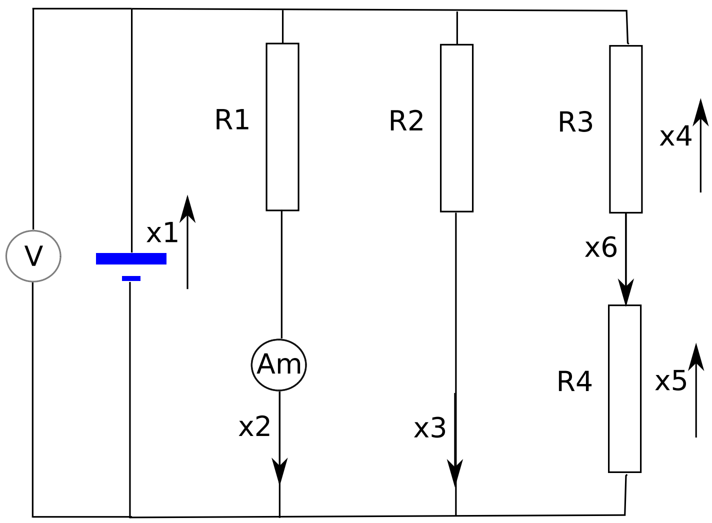


**Fig. 7** A simple electrical system (example 7)

and $Am$ respectively correspond to a voltmeter and an ammeter, which provide the relevant values $U$ and $In$. The values of the resistors $R_1, R_2, R_3, R_4$ are known and non-null. The variables $x_1$, $x_4$, $x_5$ are tensions and $x_2$, $x_3$, $x_6$ are currents. Deduced from the figure, the relevant model is system $\mathbf{A}.x = \mathbf{b}$ with

$x = \begin{pmatrix} x_1 & x_2 & x_3 & x_4 & x_5 & x_6 \end{pmatrix}^t$, $\mathbf{b} = \begin{pmatrix} U & 0 & In & 0 & 0 & 0 & 0 \end{pmatrix}^t$ and

$$\mathbf{A} = \left(\begin{array}{|rr|r|rrr|}
\hline
1 & 0 & 0 & 0 & 0 & 0 \\
-1 & R_1 & 0 & 0 & 0 & 0 \\
0 & 1 & 0 & 0 & 0 & 0 \\
\hline
-1 & 0 & R_2 & 0 & 0 & 0 \\
\hline
-1 & 0 & 0 & 1 & 1 & 0 \\
0 & 0 & 0 & -1 & 0 & R_3 \\
0 & 0 & 0 & 0 & -1 & R_4 \\
\hline
\end{array}\right)$$

Obtained after a classification of the relations and variables described in Section 4.3.1, matrix **A** presents a specific triangular structure allowing three resolutions, which are almost autonomous. Indeed, the resolution of $x_{1,}x_2$ needs only the three first relations. Then, knowing $x_{1,}$ the value of $x_3$ can be deduced with the fourth relation. Similarly, $x_4$, $x_5$, $x_6$ can be computed with the three last relations knowing $x_1$. Therefore, a sequential resolution considering subsystems and not the complete system can be made.

- Another remark is that there are two ways to deduce $x_{1,}x_2$ in the first substructure: the resolution of $x_{1,}x_2$ is named *over-determined*. In fact, only two relations are necessary: one of the three relations is redundant and can be removed. Moreover, exploiting this redundancy, we can deduce the equality $U = R_1.In$ and another point of view is to exploit this relation in fault detection. Indeed, if a sensor is faulty or the resistor is degraded or burnt, then $U \neq R_1.In$ as $U$ and $In$ are known and we can deduce that a fault has occurred in this part of the electrical system. This technique is a well-known approach of fault detection [12] [13] for continuous systems.

- As there is a unique way to deduce $x_{3,}x_4$, $x_5$, $x_6$ in the second and third substructures, the relevant resolution is named *just-determined*.

- Now, if we assume that $R_4$ is unknown in the last substructure, then the last relation cannot be used and $x_4$, $x_5$, $x_6$ cannot be computed: this resolution is called *under-determined*. ■

In fact, this example, which highlights three main situations of resolution corresponds to the three main substructures of the canonical decomposition of Dulmage-Mendelsohn developed in graph theory [17] [18]. The structural approach can be applied to continuous systems taken from different domains (electrical, mechanical, hydraulic, acoustical, thermodynamic,...) or a mix of these domains.

# 10 Declarations

## 10.1 Ethical Approval

Not Applicable

## 10.2 Availability of supporting data

Not Applicable

## 10.3 Competing interests

Not Applicable


## 10.4 Funding

Not Applicable


## 10.5 Authors' contributions

Not Applicable

## 10.6 Acknowledgments

Not Applicable

# References

[1] F. Basile, P. Chiacchio and G. De Tommasi, "On K-diagnosability of Petri nets via integer linear programming," Automatica, Volume 48, Issue 9, pp. 2047-2058, 2012.

[2] A. Chouchane, P. Declerck, A. Khedher and A. Kamoun, "Diagnostic based on estimation using linear programming for partially observable Petri nets with indistinguishable events," International Journal of Systems Science: Operations & Logistics, Taylor & Francis, pp. 1-14, 2018.

[3] A. Chouchane et P. Declerck, Diagnosis on a sliding horizon for partially observable Petri nets, Kybernetika, International journal of Institute of Information Theory and Automation of The Czech Academy of Science, Vol. 58, Number 4 , Pages 479-497, 2022.

[4] P. Bonhomme, "Decentralized state estimation and diagnosis of P-time labeled Petri nets systems," Journal of Discrete Event Dynamic Systems, 31(1), pp. 137-162, 2021.

[5] T. Becha, R. Kara, S. Collart-Dutilleul, and J. J. Loiseau, "Modelling, Analysis and Control of Electroplating Line Modelled by P-Time Event Graphs," in Proc. 6th International Conference on Management and Control of Production and Logistics, Fortaleza, Brazil, pp. 311-316, Sep. 11-13, 2013.

[6] P. Bunus, P. Fritzson, "Methods for structural analysis and debugging of modelica models," in Proc. $2^{nd}$ International Modelical Conference, pp.157-165, 2002.

[7] J.-M. Cane, A. Kubicki, D. Michelucci, H. Barki, S. Foufou, "Re-paramétrisation et réduction des systèmes irréductibles," Revue électronique Francophone d'Informatique Graphique, Vol. 8, Number 2, pp. 79-91, 2014.

[8] P. Declerck and P. Bonhomme, "State Estimation of Timed Labeled Petri Nets with Unobservable Transitions," IEEE Transactions on Automation Science and Engineering, Special Issue on Discrete Event Systems for Automation, Vol. 11, No. 1, ITASC9, pp. 103-110, January 2014.

[9] P. Declerck, "Counter approach for the estimation of optimal sequences in Partially Observable Untimed Petri Nets," Journal of Discrete Event Dynamic Systems, 2021.

[10] P. Declerck and P. Bonhomme, "Two-staged Approach for Estimation of sequences in Partially Observable P-time Petri Nets on a sliding horizon with schedulability analysis," International Journal of Control, 2023.

[11] P. Declerck, "Offline analysis of the relaxed upper boundedness for online estimation of optimal event sequences in Partially Observable Petri Nets," Journal of Discrete Event Dynamic Systems, 2024.

[12] P. Declerck and M. Staroswiecki, "Identification of structurally solvable subsystems for the design of Fault Detection and Isolation Schemes, using the Embedding Procedure," 9th IFAC/IFORS Symposium on Identification and System Parameter Estimation, pp. 230-235, Vol.1, Budapest, Hungary, July 8-12, 1991.

[13] P. Declerck and M. Staroswiecki, "Characterization of the Canonical Components of a Structural Graph for Fault Detection in Large Scale Industrial Plants," First European Control Conference, ECC'91, pp. 298-303, Vol.1, Grenoble, France, July 2-5, 1991.

[14] F. Defossez, S. Collart-Dutilleul and P. Bon, "Temporal requirements checking in a safety analysis of railway systems," FORMS/FORMAT 2008, Symposium on Formal Methods for Automation and Safety in Railway and Automotive Systems, TU Braunschweig and Budapest University of Technology and Economics, October, 2008.

[15] A.Dideban, H. Zeraatkar, Petri Net controller synthesis based on decomposed manufacturing models, ISA Transactions, pp. 1-10, 2018.

[16] M. Dotoli, M. P. Fanti and A. M. Mangini, "Fault detection of discrete event systems by Petri nets and integer linear programming," Automatica, 45(11), pp. 2665-2672, 2009.

[17] A. L. Dulmage and N. S. Mendelsohn, Covering of bipartite graphs, Canadian J. Math, 10, pp. 517-534, 1958.

[18] A. L. Dulmage and N. S. Mendelsohn, "A structure theory of bipartite graphs of finite exterior dimension," Trans. of Royal Soc. Canada, Section III, 53, pp. 1-13, 1959.

[19] E. Frisk, A. Bregon, J. Aslund, M. Krysander, B. Pulido and G. Biswas, " Diagnosability Analysis Considering Causal Interpretations for Differential Constraints," IEEE transactions on systems, man and cybernetics. Part A. Systems and humans, (42), 5, pp. 1216-1229, 2012.

[20] S. P. Hostettler, A. Linard, M. Marechal, A. Ayar and M. Risoldi, Improving the significance of benchmarks for Petri nets model checkers, In: Proceedings of the workshops APNOC and SUMo, pp. 97–111 Braga, Portugal, June 22, 2010.

[21] H. Khorasgani and G. Biswas, Structural Fault Detection and Isolation in Hybrid Systems, IEEE Transations on Automation Science and Engineering, 2017.

[22] N. Kita, Nonbipartite Dulmage-Mendelsohn Decomposition for Berge Duality. In: Wang, L., Zhu, D. (eds) Computing and Combinatorics. COCOON 2018. Lecture Notes in Computer Science(), vol 10976. Springer, 2018.

[23] J. Komenda, S. Lahaye, J-L. Boimond and T. van den Boom, "Max-plus algebra in the history of discrete event systems," Annual Reviews in Control 45, pp. 240-249, 2018.

[24] Liang Li, Yaqiong Li, Bin Liu and Weimin Wu. "Least-Cost Transition Sequence Estimation in Labeled Time Petri Net Systems with Unobservable Transitions," International Journal of Control, pp 1-14, 2022.

[25] C. Mahulea, C. Seatzu, M. Cabasino, and M. Silva, "Fault Diagnosis of Discrete-Event Systems Using Continuous Petri Nets," IEEE Transactions on Systems, Man, and Cybernetics, Vol.42, pp 970-984, 2012.

[26] K. Murota, "Systems Analysis by Graphs and Matroids. Structural solvability and controllability," Algorithms and Combinatorics 3, Springer-Verlag, 1987.

[27] R. Parker, B. Nicholson, J. Siirola and L. Biegler, Applications of the Dulmage–Mendelsohn decomposition for debugging nonlinear optimization problems, Computers & Chemical engineering, Volume 178, October 2023.

[28] A. Pothen and C.-J. Fan, "Computing the Block Triangular Form of a Sparse Matrix," ACM Transactions on Mathematical Software, Vol. 16, No. 4, pp. 303-324, December 1990.

[29] N. Ran & J. Hao & C. Seatzu, Prognosability Analysis and Enforcement of Bounded Labeled Petri Nets, IEEE Transactions on Automatic Control, pp. 1-1, 2021.

[30] N. Ran & T. Li & Z. He & C. Seatzu, Codiagnosability Enforcement in Labeled Petri Nets, IEEE Transactions on Automatic Control, Vol. 68. pp. 2436-2443, 2023.

[31] R. Wiśniewski, A. Costa, M. Wojnakowski, M. Maliński, Decomposition of a Petri Net-Based Cyber-Physical System toward Implementation as an Integrated System within FPGA, Applied Sciences, , 13, 7137, 2023.

[32] R. Wiśniewski, Ł. Stefanowicz, A. Bukowiec, and J. Lipiński, Theoretical Aspects of Petri Nets Decomposition Based on Invariants and Hypergraphs, Multimedia and Ubiquitous Engineering, Lecture Notes in Electrical Engineering 308, Springer-Verlag Berlin Heidelberg 2014.

[33] H. Yue, S. Xu, G. Zhou, H. Hu, Y. Guo, and J. Zhang, "Estimation of least-cost transition firing sequences in labeled Petri nets by using basis reachability graph," IEEE Access, PP(99):1-1, 2019.

[34] D. Zaitsev, Clans of Petri Nets: Verification of protocols and performance evaluation of networks, Publisher: Lap Lambert Academic Publishing, 278 pages, June 2013.

[35] D. Zaitsev, Sequential composition of linear systems' clans, Information Sciences, 363, pp. 292–307, 2016.

[36] D. Zaitsev, I. Zaitsev and T. Shmeleva, Infinite Petri Nets: Part 2, Modeling Triangular, Hexagonal, Hypercube and Hypertorus Structures, Complex Systems, Volume 26, Issue 4, 2017.